ISSN 2007-9737

Effect of the Trivalent Erbium Concentration on the Luminescent Properties of TiO_2 Er^{3+} Composites

Octavio Olvera-R[1], Karely Chamé-F[1], J.J. Sánchez-Mondragón[2], M. Torres Cisneros[3], M. Luisa Ojeda[1], Celso Velásquez[1]

[1] Universidad de Guadalajara,
Centro de Investigación en Nanociencia y Nanotecnología,
Mexico

[2] Instituto Nacional de Astrofísica, Óptica y Electrónica,
Óptica Cuántica,
Mexico

[3] Universidad Autónoma de Guanajuato,
División de Ingeniería,
Mexico

octavio.olvera@hotmail.com

Abstract. In this work we synthetized Er^{3+}-doped TiO_2 composites by means of the sol-gel method aiming to find the most emissive sample. For this optical characterization we used three samples with different erbium concentration (0.5, 1.0 and 3.0 wt%). We measured and compared the corresponding photoluminescent emission spectra using an excitation wavelength at 350 nm. Emission peaks in the green region associated with Er^{3+} transitions $^4S_{3/2} \rightarrow {}^4I_{15/2}$ and $^2H_{11/2} \rightarrow {}^4I_{15/2}$ were found. The sample TiO_2Er1 (1.0 wt%) had the highest intensity profile and therefore we performed further characterizations on this composite. We measured its emission spectrum in the infrared region using the same excitation at 350 nm and we found emission peaks associated with transitions $^4I_{11/2} \rightarrow {}^4I_{15/2}$ and $^4I_{13/2} \rightarrow {}^4I_{15/2}$. We verified the morphology and structural properties of this material with Raman spectroscopy, X-Ray Diffraction and Scanning Electronic Microscopy. We consider that this composite could have promising potential in applications in communications.

Keywords. Fluorescent and luminescent materials, optical properties, rare-earth-doped materials.

1 Introduction

New materials in the nanometric range are synthetized every day in order to achieve adequate properties for particular applications. These materials may include oxides as host matrices and trivalent rare-earths (RE) as dopants. Semiconductor titanium dioxide (TiO_2) is an ideal host for RE emitters due to its good optical and thermal properties and this combination has been used intensively in the last years [1-10]. Among RE erbium (Er) is probably the most used due to its emission properties in applications such as fiber amplifiers, communications, display devices and sensors [11-16]. Emission bands for the Er^{3+} are well-known both in the visible and in the infrared (IR) ranges. In particular, a useful and well-studied emission band is that located around 1550 nm which has maximum transmittance and minimum losses.

In this paper, we report the synthesis and characterization of a promising Er^{3+}-doped TiO_2 composite that showed adequate photoluminescence (PL) emission properties both in the visible and IR ranges. To define the optimal dopant concentration for the PL emission we varied the Er^{3+} amount (0.5, 1.0 and 3.0 wt%) aiming to determine the most emissive sample in the visible region.

By comparing the obtained emission spectra, we determined that the sample with 1.0 wt%,

ISSN 2007-9737

denoted as TiO_2Er1, had the highest intensity profile. Therefore, in the successive we characterized only this sample.

We measured the PL emission spectrum in the IR range and strong emission around 1550 nm was found. We also verified the morphology and structural properties of our composite with Raman spectroscopy, X-Ray Diffraction and Scanning Electronic Microscopy. All the composites were synthetized with the sol-gel and Stöber methods.

2 Experimental

2.1 Reagents

All chemicals are of analytical grade and are used as received without any further purification. Titanium(IV) isopropoxide $Ti[OCH(CH_3)_2]_4$ purity 97%, penta-hydrated erbium nitrate $Er(NO_3)_3\ 5H_2O$ and potassium chloride KCl ($4x10^{-4}$ M) purity 99.9 % were purchased from Aldrich. Ethanol purity 99.9% was purchased from Sigma.

2.2 Synthesis of TiO_2 Er^{3+} Composites

We synthetized our composites with the sol-gel and the Stöber methods. All conditions were the same for the three samples with the exception of the amount of erbium nitrate used. Herein we provide the description for the sample TiO_2Er1. 56 mg of penta-hydrated erbium nitrate, 26.66 ml of ethanol and 0.106 ml of potassium chloride 0.4 mM were poured into a volumetric flask under a low humidity atmosphere.

The solution was stirred vigorously and the temperature was increased to 50 °C. At this temperature, we started to drop 1.92 ml of titanium isopropoxide at a rate of one drop every two minutes. When finished the system was vigorously stirred for 18 hours at 50° C.

Then the remaining ethanol was removed and a gel was formed. This was heated for two hours at 80° C and it was solidified. The solid obtained was pulverized and calcined under a nitrogen atmosphere for three hours at 700°C.

As mentioned, this sample was labeled as TiO_2Er1, while the other samples were labeled as TiO_2Er05 and TiO_2Er3 for 0.5 and 3.0 wt%, respectively.

2.3 Characterization

The PL measurements in the visible range were performed on a Varian Cary Eclipse fluorescence spectrophotometer equipped with a xenon lamp. The corresponding measurements in the IR range were carried out on an Edinburgh Instruments fluorescence spectrophotometer using an InGaAs photo-detector.

Raman spectroscopy was performed on a Raman Thermo Scientific instrument equipped with a laser beam of 633 nm. XRD patterns were obtained on a Bruker D8 Advance diffractometer working at 40 Kv and 35 MA. SEM images were obtained with a JSM 6610LV Scanning Electron Microscope 30 KV magnification x 5 to x 300,000 (on 128 mm x 96 image-size).

3. Results and Discussion

3.1 Optical Properties

In Fig. 1 we show the PL excitation spectrum for the sample TiO_2Er1 in the range 290-450 nm by using an emission wavelength at 550 nm. The curve has a maximum around 350 nm, which is associated with transition $^4I_{15/2} \rightarrow {}^4G_{7/2}$ [17] with an energy around 28 500 cm^{-1}. This value was used as the excitation wavelength for the emission spectra.

In Fig. 2 we show the emission spectra obtained for the three samples in the range 450-600 nm by using the excitation wavelength at 350 nm. We found strong emissions with peaks centered at 495, 520 and 553 nm.

The first two peaks are associated with erbium transition $^2H_{11/2} \rightarrow {}^4I_{15/2}$ while the last one is associated with transition $^4S_{3/2} \rightarrow {}^4I_{15/2}$ [6, 10, 17-20]. It can be seen that intensity increases notably when Er^{3+} concentration increases from 0.5 to 1 wt%.

However when we keep increasing concentration up to 3 wt% we found a quenching in the PL intensity. This might be due to energy transfer (ET) mechanisms associated with a saturation of the Er^{3+} ions, where the distance between neighbors decreases drastically as we increase concentration.

ISSN 2007-9737

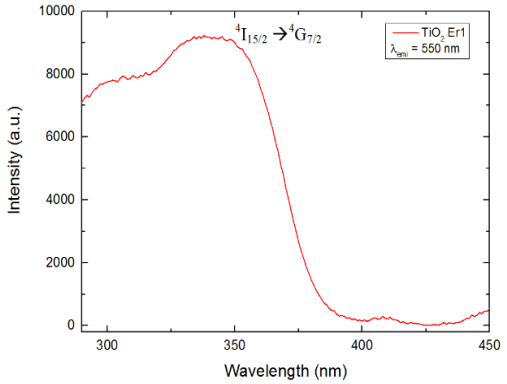

Fig. 1. PL excitation spectrum for the TiO_2Er1 composite with an emission wavelength at 550 nm

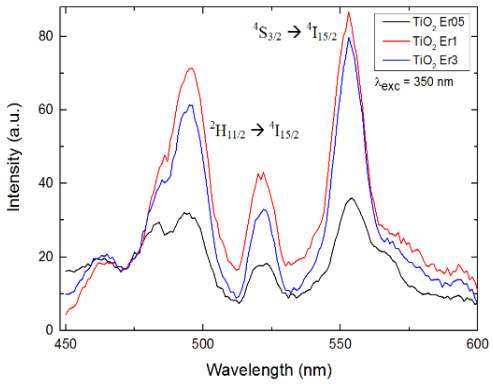

Fig. 2. PL emission spectra in the visible range (450-600 nm) for the TiO2 composites with different Erconcentrations (0.5, 1.0 and 3.0 wt%) with an excitation wavelength at 350 nm. Peaks association is described in the text

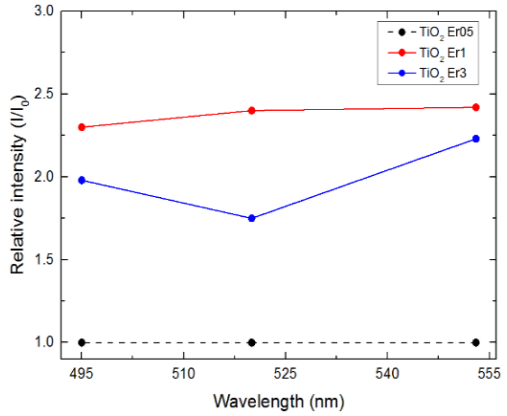

Fig. 3. Relative intensities for the TiO_2 Er1 and TiO_2 Er3 composites with respect to TiO_2 Er05 composite. Description is provided in the text.

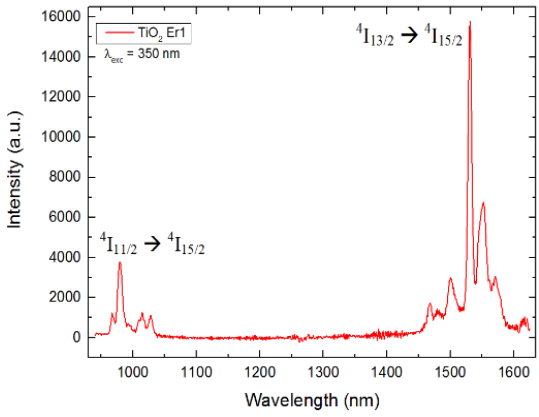

Fig. 4. PL emission spectrum in the infrared range (940-1625 nm) for the TiO2 Er1 composite with an excitation wavelength at 350 nm. Peaks association is described in the text.

This feature may be useful for up-conversion (UC) studies, but is beyond the scope of this manuscript.

In Fig. 3 we show the relative intensities with respect to the sample TiO_2Er05 (minimum intensity, represented by the black dashed line). Red dots represent the ratio I_{Er1}/I_{Er05} for the three wavelengths where the peaks were located (495, 520 and 553 nm).

Blue dots correspond to the ratio I_{Er3}/I_{Er05}. Solid lines were included to facilitate the comparison. It can be seen that the intensity profile for TiO_2Er1 is 2.25-2.5 times higher than the corresponding intensity for TiO_2Er05. TiO_2Er3 shows lower values, between 1.75-2.25 times higher. After comparison from Fig. 3 we determined that sample TiO_2Er1 is the most adequate for further characterizations.

In Fig. 4 we show the PL emission spectrum for TiO_2Er1 in the IR range, from 940 to 1625 nm. We found peaks around 980 nm which are associated with the transition $^4I_{11/2} \rightarrow {}^4I_{15/2}$ and a strong emission around 1531 nm associated with transition $^4I_{13/2} \rightarrow {}^4I_{15/2}$ [17, 21-23].

ISSN 2007-9737

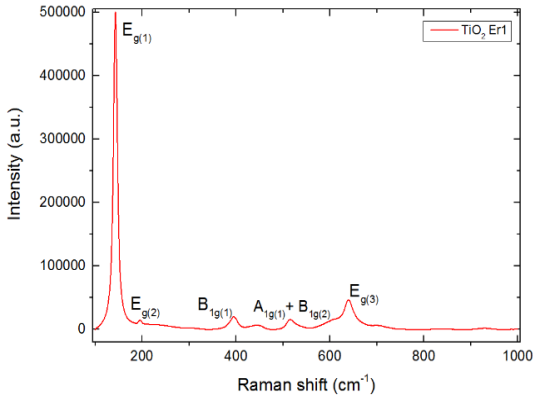

Fig. 5a. Raman spectrum for the TiO2Er1 sample. The peaks association is described in the text

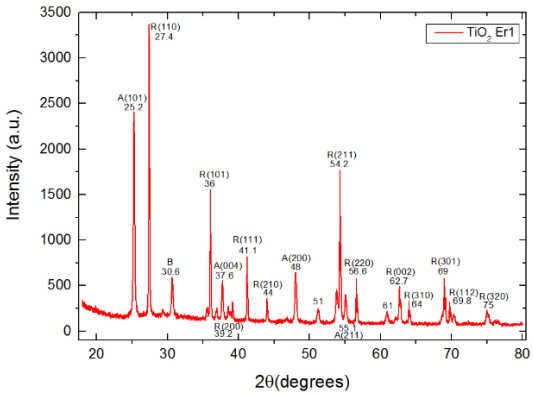

Fig. 5b. XRD spectrum for the TiO2Er1 sample. In the association of the peaks we found a combination of rutile, anatase and brookite crystalline phases Peaks association is described in the text

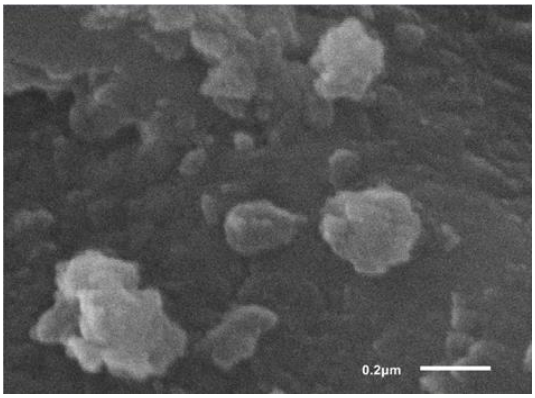

Fig. 5c. SEM image for the TiO2Er1 sample. The diameter for the crystals is in the range 100-400 nm

3.2 Crystal Structure and Morphology

Fig. 5 shows the characterizations performed for the structure and morphology of the TiO_2Er1 composite.

Fig. 5a shows the Raman spectrum obtained. The peaks shown are the phonon modes associated with the anatase phase [1-3, 6, 9-10].

The 143 cm^{-1} associated with $E_{g(1)}$ mode, 196 cm^{-1} with $E_{g(2)}$, 395 cm^{-1} with $B_{1g(1)}$, 515 cm^{-1} with $A_{1g(1)}$+$B_{1g(2)}$ and 639 cm^{-1} with $E_{g(3)}$.

Fig. 5b shows the XRD spectrum obtained. We associated a total of 17 peaks [1, 7] as follows: 12 peaks with the rutile phase: 27.4º with R(110), 36º with R(101), 39.2º with R(200), 41.1º with R(111), 44º with R(210), 54.2º with R(211), 56.6º with R(220), 62.7º with R(002), 64º with R(310), 69º with R(301), 69.8º with R(112) and 75º with R(320); 4 peaks with the anatase phase: 25.2º with A(101), 37.6º with A(004), 48º with A(200) and 55.1º with A(211) and finally one peak at 30.6° associated with the brookite phase.

Fig. 5c shows a SEM image obtained. The diameter for the crystals is in the range 100-400 nm.

4 Conclusions

We synthetized three Er^{3+}-doped TiO_2 composites with different erbium concentration (0.5, 1.0 and 3.0 wt%) with the sol-gel method. In order to find the most emissive sample we measured and compared the photoluminescent emission spectra using an excitation wavelength at 350 nm.

We found three main peaks in the green region associated with Er^{3+} transitions $^4S_{3/2}$ → $^4I_{15/2}$ and $^2H_{11/2}$→ $^4I_{15/2}$. We determined that the sample TiO_2Er1 (1.0 wt%) had the highest intensity profile and then we performed further characterizations on this composite. We also measured its photoluminescent emission spectrum in the infrared region using the same excitation at 350 nm and we found strong emission peaks associated with transitions $^4I_{11/2}$ → $^4I_{15/2}$ and $^4I_{13/2}$ → $^4I_{15/2}$. The most intense peak located at 1531 nm corresponds to the well-known window used in communications and fiber amplifiers due to its maximum transmittance. Because of this, we consider that

this composite could have promising potential in applications in those fields.

References

1. **Palomino-Merino, R., Trejo-Garcia, P., Portillo-Moreno, O., Jiménez-Sandoval, S., Tomás, S. A., Zelaya-Angel, O., Lozada-Morales, R., & Castaño. V.M. (2015).** Red shifts of the $E_{g(1)}$ Raman mode of nanocrystalline TiO_2:Er monoliths grown by sol–gel process. *Optical Materials,* Vol. 46, pp. 345–349. DOI: 10.1016/j.optmat.2015.04.042.
2. **Lubas, M., Jasinski, J. J., Sitarz, M., Kurpaska, L. Podsiad, P., & Jasinski, J. (2014).** Raman spectroscopy of TiO2 thin films formed by hybrid treatment for biomedical applications. Spectrochimica Acta Part A: Molecular and Biomolecular Spectroscopy. *Advisory Board,* Vol.133, pp. 867–871. DOI: 0.1016/j.saa.2014. 05.045.
3. **Gaintantzopoulou, M., Zinelis, S., Silikas, N., & Eliades. G. (2014)**. Micro-Raman spectroscopic analysis of TiO_2 phases on the root surfaces of commercial dental implants. *Dental Materials,* Vol. 30, pp. 861–867. DOI: 10.1016/j.dental.2014.05.030.
4. **Zhao, J., Feng, J., Xie, E., Zhao, A., & Liu, Z. (2011).** Visible erbium luminescence in Er^{3+}-doped SiO_2-TiO_2 films prepared by sol-gel method. *Journal of optoelectronics and advanced materials,* Vol. 13, No. 5, pp. 466–470.
5. **Luo, W., Fu, C., Li, R., Liu, Y., Zhu, H., & Chen, X. (2011).** *Er^{3+}-Doped Anatase TiO_2 Nanocrystals: Crystal-Field Levels.* Excited-State Dynamics, Upconversion, and Defect Luminescence. Small, Vol. *7,* No. 21, pp. 3046–3056. DOI: 10.1002/ smll.201100838.
6. **Badr, Y., Battisha, I. K., Salah, A., & Salem, M. A. (2008).** *Up-conversion luminescence application in Er^{3+}:TiO_2 thin film prepared by dip coating sol-gel route.* Indian Journal of Pure & Applied Physics, Vol. 46, pp. 706–711.
7. **Pal, M., García-Serrano, J., Santiago, P., & Pal, U. (2007).** Size-Controlled Synthesis of Spherical TiO_2 Nanoparticles: Morphology, Crystallization, and Phase Transition. *The Journal. of Physical Chemistry*, Vol. 111, No. 1, pp. 96–102. DOI: 10.1021/jp0618173.
8. **Jeon, S. & Braun, P. V. (2003).** Hydrothermal synthesis of Er-doped luminescent TiO_2 nanoparticles. *Chemistry of Materials*, Vol. 15, No. 6, pp. 1256–1263. DOI**:** 10.1021/cm0207402.
9. **Bahtat, A., Bouderbala, M., Bahtat, M., Bouazaoui, M., Mugnier, J., & Druetta, M. (1998).** Structural characterisation of Er^{3q} doped sol–gel TiO_2 planar optical waveguides. *Thin Solid Films*, Vol. 323, pp. 59–62.
10. **Bahtat, A., Bouazaoui, M., Bahtat, M., Garapon, C., Jacquier, B., & Mugnier, J. (1996).** Up-conversion fluorescence spectroscopy in Er^{3+}:TiO_2 planar waveguides prepared by a sol-gel process. *Journal of Non-Crystalline Solids*, Vol. 202, pp. 16-22. DOI: 10.1016/0022-3093(96)00172-X.
11. **Zhang, M., Zhang, W., Wang, F., Zhao, D., Qu, C., Wang, X., & Zhang, D. (2016).** High-gain polymer optical waveguide amplifiers based on core-shell $NaYF_4$/$NaLuF_4$: Yb^{3+}, Er^{3+} NPs-PMMA covalent-linking nanocomposites*. Scientific reports*, Vol. 6. DOI: 10.1038/srep36729.
12. **Ye, H. Q., Li, Z., Peng, Y., Wang, C. C., Li, T. Y., Zheng, Y. X., & Gillin, W. P. (2014).** Organo-erbium systems for optical amplification at telecommunications wavelengths. *Nature materials,* Vol. 13, No. 4, pp. 382–386. DOI: 10.1038/ NMAT3910.
13. **Zannen, M., Dietze, M., Khemakhem, H., Kabadou, A., & Es-Souni, M. (2014).** The erbium's amphoteric behavior effects on sodium bismuth titanate properties. *Ceramics International*, Vol. 40 No. 8, pp. 13461–13469. DOI: 10.1016/j.ceramint. 2014.05.069.
14. **Tanabe, S. (1999).** Spectroscopic studies on multiphoton processes in erbium doped fluoride and oxide glasses. *Journal of non-crystalline solids*, Vol. 256, pp. 282–287. DOI: 10.1016/S0022-3093 (99)00466-4.
15. **Polman, A. (1997).** Erbium implanted thin film photonic materials. *Journal of Applied Physics*, Vol. 82, No. 1, pp. 1–39. DOI: 10.1063/1.366265.
16. **Ohtsuki, T., Honkanen, S., Najafi, S. I., & Peyghambarian, N. (1997)** *Cooperative upconversion effects on the performance of Er^{3+}-doped phosphate glass waveguide amplifiers.* JOSA B, Vol. 14, No. 7, pp. 1838–1845. DOI: 10.1364 /JOSAB.14.001838.
17. **Mears, R. J., Reekie, L., Jauncey, I. M., & Payne, D. N. (1987).** Low-noise erbium-doped fibre amplifier operating at 1.54 μm. *Electronics Letters*, Vol. 23, No. 19, No. 1, pp. 026–1028. DOI: 10.1049/el:19870719.
18. **Carnall, W. T., Crosswhite, H., & Crosswhite, H. M. (1978).** *Energy level structure and transition probabilities in the spectra of the trivalent lanthanides in LaF_3.*
19. **Tsao, H. X., Lin, S. T., Wang, C. L., Su, H. C., Huang, C. M., Jhang, Y. W., & Sheu, J. K. (2012).**

A green upconversion laser with erbium-doped LiLuF 4 crystal by 976 nm fiber laser pump. *International Journal of Optics and Applications*, Vol. 2, No. 5, pp. 72–75. DOI: 10.5923/j.optics.20120205.03.

20. **Gouveia, E. A., de Araujo, M. T., & Gouveia-Neto, A. S. (2001).** Thermal Effects on Light Emission in Yb^{3+}-Sensitized Rare-Earth Doped Optical Glasses. *Brazilian Journal of Physics*, Vol. 31, No. 1. DOI: 10.1590/S0103-97332001000100017.
21. **Mahraz, Z. A. S., Sahar, M. R., Ghoshal, S. K., & Dousti, M. R. (2013).** Concentration dependent luminescence quenching of Er^{3+}-doped zinc borotellurite glass. *Journal of luminescence*, Vol. 144, pp. 139–145. DOI: 10.1016/j.jlumin.2013.06.050.
22. **Awang, A., Ghoshal, S. K., Sahar, M. R., Dousti, M. R., Amjad, R. J., & Nawaz, F. (2013).** Enhanced spectroscopic properties and Judd–Ofelt parameters of Er-doped tellurite glass: Effect of gold nanoparticles. *Current Applied Physics*, Vol. 13, No. 8, pp. 1813–1818.
23. **Dai, S., Lu, L., Xu, T., Nie, Q., Shen, X., & Wang, X. (2007).** Optical properties of and concentration quenching in Bi_2O_3–B_2O_3–Ga_2O_3 glasses. *Journal of non-crystalline solids*, Vol. 353, No. 28, pp. 2744–2749. DOI: 10.1016/j.jnoncrysol.2007.05.018.
24. **Ling, Z., Ya-Xun, Z., Shi-Xun, D., Tie-Feng, X., Qiu-Hua, N., & Xiang, S. (2007).** Effect of Ga_2O_3 on the spectroscopic properties of erbium-doped borobismuth glasses. *Spectrochimica Acta, Part A: Molecular and Biomolecular Spectroscopy*, Vol. 68, No. 3, pp. 548–553. DOI: 10.1016/j.saa.2006.12.026.

Article received on 14/09/2018; accepted on 04/12/2018.
Corresponding author is Octavio Olvera-R.